*Aerosol and Air Quality Research*, 17: 2224–2234, 2017

ISSN: 1680-8584 print / 2071-1409 online
doi: 10.4209/aaqr.2017.06.0207

# Characteristics and source Analysis of trace Elements in $PM_{2.5}$ in the Urban Atmosphere of Wuhan in Spring

**Costanza Acciai[1], Zhenyi Zhang[1,2*], Fenjuan Wang[1,2*], Zhangxiong Zhong[4], Giovanni Lonati[1]**

[1] *Department of Civil and Environmental Engineering, Politecnico di Milano, Milan 20133, Italy*
[2] *INET, Tsinghua University, Beijing 100084, China*
[3] *National Climate Center, China Meteorological Administration, Beijing 100081, China*
[4] *Wuhan Environmental Monitoring Center, Wuhan, HuBei 430015, China*

## ABSTRACT

The concentrations of $PM_{2.5}$ and trace elements with hourly resolution were measured during May 2014 in urban residential area of Wuhan, the biggest city in central China. During the period of measurement, the average temperature was approximate 25°C without domestic heating and cooling. The average concentration of $PM_{2.5}$ was 95.53 μg $m^{-3}$, which was higher than the limit of Ambient Air Quality Standard of China GB3095-2012 (75 μg $m^{-3}$, Level 2). A sand storm original from Northwestern China was also recorded. Concentrations of major trace elements (K, Ca, V, Cr, Mn, Fe, Ni, Cu, Zn, Ga, As, Se, Pd, Ag, Cd, Au, Hg, Pb, Co, Sn, Sb, Tl) were comparable to previous studies, except for Ba and Ca with more than doubled concentrations (103 ng $m^{-3}$, 1,792.49 ng $m^{-3}$) due to the storm. Enrichment Factor (EF) and Positive Matrix Factorization (PMF) were employed to characterize the emission sources. The computation of EF showed that Zincs was highly enriched. Four sources, biomass burning (63.2%) might mainly related to power plants using bio-waste burning and bio-related cooking activities, metallurgical and steel industries (14%), dust crustal (12.5%) and dust associated with vehicular traffic (10.4%), were identified in decreasing order of average percentage contribution to the $PM_{2.5}$ mass with the aid of trace elements. The orientations of emission sources were also addressed.

***Keywords:*** Trace element; $PM_{2.5}$; Enrichment factor; Positive matrix factorization; Central China.

## INTRODUCTION

Air pollution influences many megacities and their surroundings worldwide (Srivastava *et al.*, 2008; Kanakidou *et al.*, 2011; Zhang *et al.*, 2012). In China, air pollution in megacities is mainly caused by the drastic economic growth, together with the rapid industrialization and the wide urbanization (e.g., Wang *et al.*, 2014a, b; Li *et al.*, 2015; Lang *et al.*, 2017). China has been suffering from serious air quality problems, mostly related to fine particulate matter (Jiang *et al.*, 2015; Lv *et al.*, 2015; San Martini *et al.*, 2015). The environmental reports indicate that only 8 of the 74 major cities meet the limit of ambient air quality standard of China (Chinese Ministry of Environmental Protection, 2015): across all major cities, the average pollutant concentrations in 2014 were 64 μg $m^{-3}$ for $PM_{2.5}$, 105 μg $m^{-3}$ for $PM_{10}$ and 42 μg $m^{-3}$ for $NO_2$, respectively. The climate effect (IPCC, 2013) and the health implications of fine particles have been well reported in the previous studies (Pope and Dockery, 2006; Cao *et al.*, 2012; Guo *et al.*, 2013; Kim *et al.*, 2015), meanwhile the high concentrations of oxidizing species were frequently observed in urban centers. However, there is still essential demand for improving knowledge in the source contributions and variation of ground-level fine particles, in order to assess the efficacy of emission mitigation strategies and to improve ambient air quality (Wang *et al.*, 2010; Xu *et al.*, 2013a).

Particulate matter (PM) is released into the atmosphere by natural sources, e.g., soil dust, volcanism, erosion, surface winds and forest fires; and by anthropogenic sources, e.g., fossil fuel combustion, industrial metallurgical processes, vehicle emissions and waste incinerations (Tian *et al.*, 2007). The geographical and meteorological conditions, such as temperature, wind speed, wind direction, pressure, etc., may influence the air pollution (Manousakas *et al.*, 2015). Typical sources of air pollution in big cities can be vehicle emissions, dust resuspension, secondary aerosol formation, industrial emissions, biomass or coal burning, power plant emissions etc. (Lu *et al.*, 2016). The characteristics of PM sources have been widely investigated in previous studies all around world, including China, as reviewed by (Karagulian *et al.*, 2015), and several methods of receptor

* Corresponding author.
*E-mail address:* zhangzhenyi@tsinghua.edu.cn (Z. Zhang); wangfj@cma.cn (F. Wang)

modeling have been used for identification and apportionment of PM (Viana *et al.*, 2008). Enrichment Factor (EF) and Positive Matrix Factorization (PMF) are widely used because they only require observation data at the receptor site other than detailed prior knowledge of the sources and source profiles, and tools to perform these analyses are widely available (Schauer, *et al.*, 2006; Yu *et al.*, 2013; Gao *et al.*, 2014; Banerjee *et al.*, 2015).

Literatures about source apportionment in central China are still very limited. It is still lacking in the study of trace elements and related source contributions of fine PM in central China. Wuhan is one of the major cities in central China, which has great competitive power for domestic trade and is regarded as China's new economic and geographic center by the domestic economists (Zhang *et al.*, 2015). In recent years, due to the dense urbanization, industrial activities and other human activities in Wuhan, such as cement processing, smelting, coal combustion and automobile emissions, the urban area has already experienced serious air quality problems. The major sources of air pollution in Wuhan may derive from the automobile exhaust and emission by using coal for domestic cooking, heating, and industrial processing (Wang *et al.*, 2014a). Six-year observation of aerosol optical properties has proved that this region is polluted by populated fine-mode particles. The mean atmospheric $PM_{2.5}$ mass concentration was about 160 ± 50 μg $m^{-3}$ (Wang *et al.*, 2012; Wang *et al.*, 2014b). Thus, it is very urgent and necessary to study the $PM_{2.5}$ source apportionment in central China in order to improve the knowledge for regional and urban air quality control.

This paper aims to study the state of PM and trace elements in Wuhan to assess the contribution of anthropogenic and natural sources. The variation characteristics of 19 elements in $PM_{2.5}$ samples were investigated using the Enrichment Factor (EF) method and Positive Matrix Factorization (PMF) method was employed to conduct the source identification and apportionment of elements in PM in order to identify the possible major sources.

## EXPERIMENTAL

### *Measurement Site*

Wuhan, the largest metropolis in central China with area of 8.494 $km^2$ and population of approximately 10.2 million, is located at the eastern part of Jianghan plain and the intersection of the Yangtze River and Hanjiang River (Zhang *et al.*, 2015). It is in the region of typical North subtropical humid monsoon climate, with annual average temperature of 15.8–17.5°C and annual average rainfall of 1050–2000 mm (Wang *et al.*, 2014), appearing the habitual condition of hot summers and cold winters with high relative humidity.

The measurement site is at the Super Monitoring Station of Wuhan (30°36'N–114°17'E), in the typical residential urban area (Fig. 1). The measurement period was from May 15$^{th}$ to May 31$^{st}$, 2014. During the period, the domestic heating and cooling with air conditioning were not generally used as the temperature was in the range of 17–34°C with average value of 25°C. The average wind speed was 1.3 m $s^{-1}$ with north-northwest as the prevailing wind direction, and wind calms occurred hourly for 24% during measurement period.

### *Instrumentation*

The hourly $PM_{2.5}$ concentration was measured using Met One Beta Attenuation Mass Monitor (Model BAM-1020) and hourly $PM_{10}$ concentration was measured using Thermal Oscillation balance monitor (TEOM Model RP1400). Elements in $PM_{2.5}$ were analyzed using the Xact 625

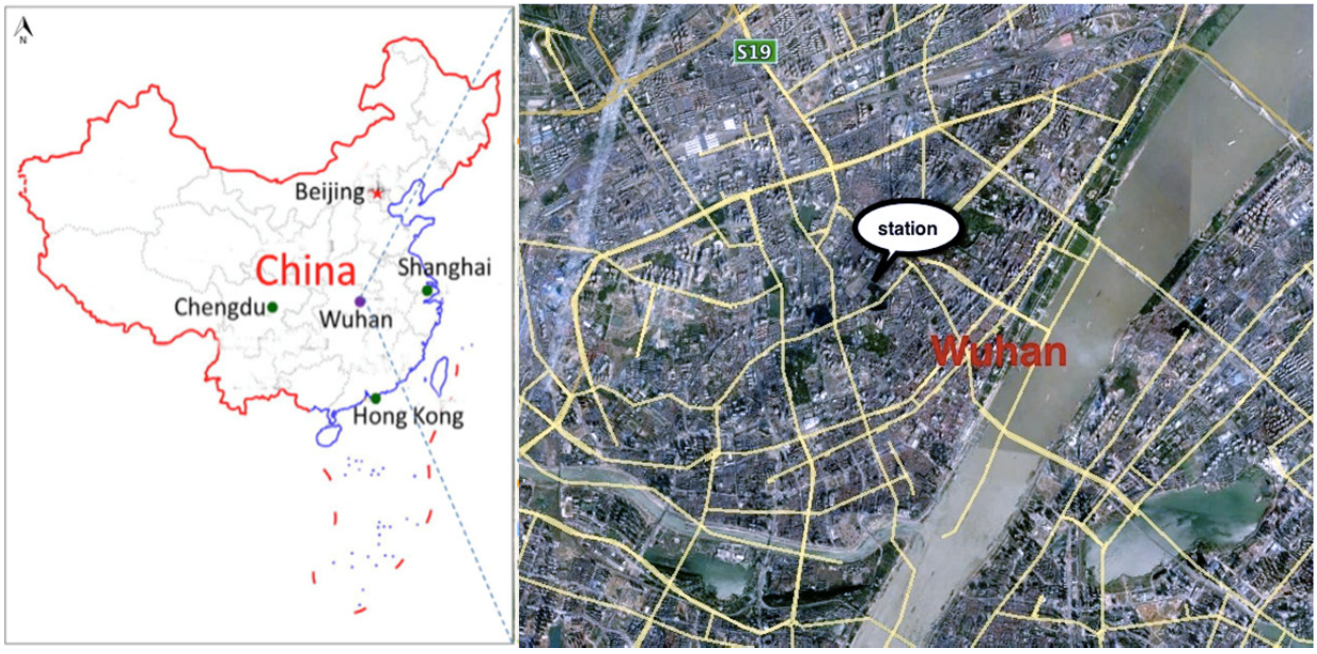


**Fig. 1.** Measurement site at Wuhan super monitoring station (map source: www.maps.google.com).

automated multi-metals monitor with the XRF (X-ray fluorescence) standard method IO3.3 of US-EPA (US-EPA). The Xact 625 monitor can analyze 23 elements (K, Ca, V, Cr, Mn, Fe, Ni, Cu, Zn, Ga, As, Se, Pd, Ag, Co, Ba, Au, Hg, Pb, Cd, Sn, Sb, Ti) with hourly resolution. In this study, four elements, Co, Sb, Sn and Ti, are equal to zero for all the time period except of some spots. Therefore, these four elements were ignored, and the remaining 19 elements were considered for further analysis.

***Enrichment Factor***

Enrichment factor (EF) analysis is employed to assess the natural and anthropogenic sources of $PM_{2.5}$ bounded elements. EF analysis helps to determine whether certain element has additional or anthropogenic sources other than its major natural sources (Lopez *et al.*, 2005). EF is defined as the ratio of considered element concentration (X) to the reference element (R) concentration for aerosol, divided by the same ratio for the Earth crust, expressed by the following equation:

$$EF = \frac{\left(\frac{X}{R}\right)_{aerosol}}{\left(\frac{X}{R}\right)_{crust}} \quad (1)$$

The value of EF less than 10 indicates that the element is mainly from crustal sources. Meanwhile the value of EF greater than 10 indicates that the element is enriched and associated with human activities (Pan *et al.*, 2013; Pan *et al.*, 2015). Si, Al (Chatterjee *et al.*, 2007) and Fe (Manoli *et al.*, 2002; Dordevic *et al.*, 2005; Samara *et al.*, 2005; Yaroshevsky, 2006) are the most common elements used as reference materials. In this study, Fe was used as the reference material and data from Mason and Morre (1982) was used for the concentrations of elements in the Earth's crust. EFs were calculated for the analysis of Ba, Ca, Cr , K, Mn, V, and Zn.

***Positive Matrix Factorization***

Positive Matrix Factorization (PMF 5.0) method is adopted to conduct the source identification and apportionment of elements in $PM_{2.5}$. The PMF model is one of the receptor models developed by US Environmental Protection Agency (US-EPA). Multivariate receptor models are very useful in the environmental studies of source apportionment of pollutants. Among them, PMF, simply requiring PM speculated data, is the most preferred and trusted one (Khan *et al.*, 2015). In this model, any data matrix X with dimension $n$ row by $m$ columns, where $n$ and $m$ are the number of samples and the number of species, can be expressed as following equations. G ($n \times p$) and F ($p \times m$) represent the two factorized matrices and E denotes the residual matrix, where $p$ is the number of factors or sources in consideration.

$$X = GF + E \quad (2)$$

or

$$x_{i,j} = \sum_{k=1}^{p} g_{i,k} f_{k,j} + e_{i,j} \quad (3)$$

where $x_{i,j}$ is the concentration of species $j$ measured on sample $i$, $p$ is the number of the factors contributing to the samples, $f_{kj}$ is the concentration of species $j$ in factor profile $k$, $g_{ik}$ is the relative contribution of factor $k$ to sample $i$ and $e_{ij}$ is error of the PMF model for the $j$ species measured in sample $i$. The goal is to find the $g_{ik}$, $f_{kj}$ and $p$ values that best reproduce $x_{i,j}$. The values of $g_{ik}$ and $f_{kj}$ are adjusted until a minimum value of $Q$ for a given $p$ is found, where $Q$ is defined as:

$$Q = \sum_{j=1}^{m} \sum_{i=1}^{n} \frac{e_{ij}^2}{s_{ij}^2} \quad (4)$$

where $s_{ij}$ is the uncertainty of the $j_{th}$ species concentration in sample $i$, $n$ is the number of samples and $m$ is the number of species.

Two input files are required by PMF: samples species concentration values and sample species uncertainty values or parameters for calculating uncertainty. According to the PMF User Guide by US EPA, in the present work, when the concentration is less than or equal to the instrumental detection limit (DL), it is substituted by half the DL and the uncertainty is calculated using the following equation (Polissar *et al.*, 1998; Yu *et al.*, 2013; Gao *et al.*, 2014):

$$Unc = \frac{5}{6} \times DL \quad (5)$$

When the concentration is greater than DL, the uncertainty is calculated according to:

$$Unc = \sqrt{\left(Error\ Fraction \times concentration\right)^2 + \left(DL\right)^2} \quad (6)$$

The DLs and the Error Fractions for 15 elements, used in calculating the uncertainties, were found in the guide of the instrument (Xact 625 Guide, US-EPA). Missing data were substituted with the median value and their uncertainties were replaced by four time the median values. We included the $PM_{2.5}$ mass concentration in order to have relative mass contribution fraction of different sources, which was assigned as a Total Variable in PMF setup.

## RESULTS AND DISCUSSION

***Concentrations of PM and Trace Elements***

The temporal variation of $PM_{10}$ and $PM_{2.5}$ during the monitoring period in May 2014 are depicted in Fig. 2.

For both $PM_{10}$ and $PM_{2.5}$, the concentration time pattern can be divided into three subsets: from May 15$^{th}$ to May 21$^{st}$, from May 22$^{nd}$ to May 25$^{th}$, and from May 26$^{th}$ to the end of the month, respectively. In the first period, the concentration of $PM_{2.5}$ oscillates between a minimum value

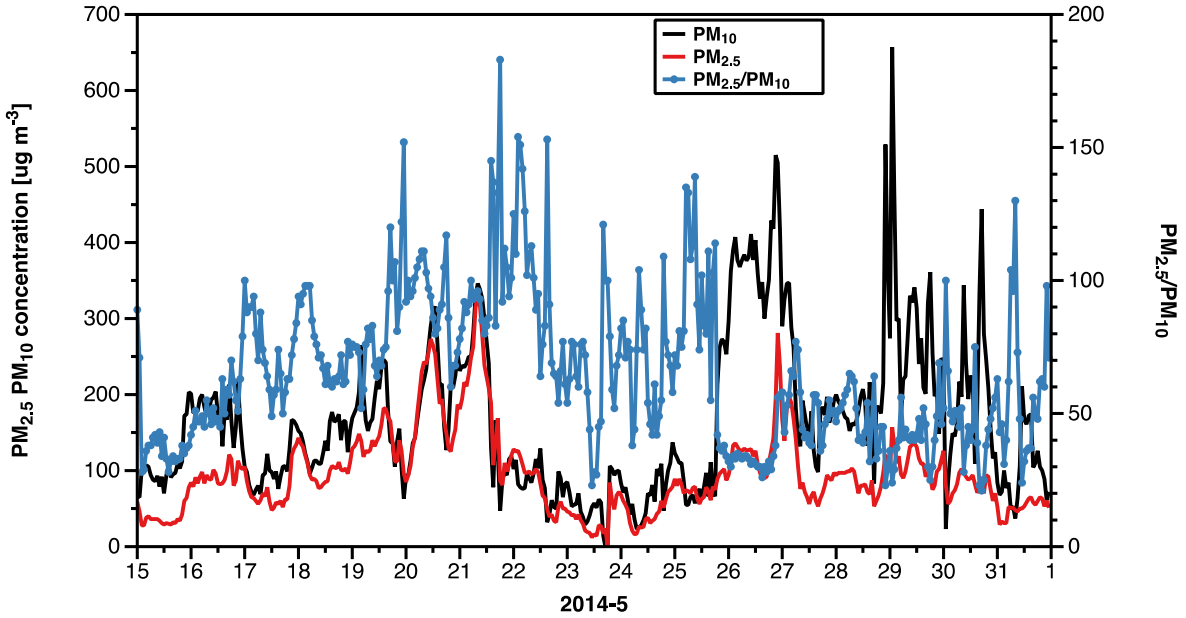


**Fig. 2.** Penetration efficiencies of the dust-mist (a) and N95 (b)

of 30 μg $m^{-3}$ and a maximum value of 330 μg $m^{-3}$, with an average of 120 μg $m^{-3}$, while $PM_{10}$ are in the range of 50–350 μg $m^{-3}$, with an average of 160 μg $m^{-3}$. Both size cuts show a progressive increase in the concentration levels, leading to the maximum values recorded on May 21st. At the beginning of the second period, the concentrations of $PM_{2.5}$ and $PM_{10}$ sharply decreased as the consequence of the precipitation event occurred on May 22th and 23th, and then remained fairly constant. The maximum values in this period are respectively 130 μg $m^{-3}$ and 270 μg $m^{-3}$ while the average decrease to 60 μg $m^{-3}$ and 80 μg $m^{-3}$. At the very beginning of the last period on May 26th, the concentration of $PM_{10}$ increased rapidly (about 300 μg $m^{-3}$ within a few hours) while $PM_{2.5}$ showed a less relevant increase; however, at the end of the day $PM_{10}$ rised up to 520 μg $m^{-3}$ and $PM_{2.5}$ up to 280 μg $m^{-3}$, and they both rapidly decreased and remained stable for the next two days. The reason for such behavior is very likely a sandstorm that brought desert dust down to Southern China. Indeed, Asian dust events are quite common in China in spring (Yu *et al.*, 2013), with dust storm travelling from the Taklamakan desert in Northwestern China and Inner Mongolia BadanJaran desert and TengKoErh desert in Northern part of China towards the Eastern and Southern regions of China together with dry air masses. For this specific event, $PM_{10}$ peak concentrations progressively decreased along the route of the storm, with hourly average that exceeded 2000 μg $m^{-3}$, 1000 μg $m^{-3}$ and 600 μg $m^{-3}$ in Lanzhou, Yinchuan and Wuhan, respectively (Wang *et al.*, 2015). The arrival of the dust storm in Wuhan on May 26th, is traced by the decrease of the average relative humidity that drops from about 80% on the previous days down to about 50%, coherently with the origin of the dust event, coarse particles are dominant and $PM_{10}$ concentration increases more pronouncedly than $PM_{2.5}$: the average of $PM_{10}$ is 230 μg $m^{-3}$ while the average of $PM_{2.5}$ is 90 μg $m^{-3}$.

Another fast increase of $PM_{10}$ is observed on the early hours of May 29th, when $PM_{10}$ reaches the highest value of the whole monitoring period (660 μg $m^{-3}$), and rather large fluctuations are observed in the following hours until the end of the monitoring period. Concurrently, $PM_{2.5}$ shows less relevant variability, with concentration levels lower than 100 μg $m^{-3}$.

The three sub-periods are also characterized by different behaviors of the mass ratio between $PM_{2.5}$ and $PM_{10}$. Actually, during the first two periods (from the start of sampling to May 21st and from May 22th to May 25th), the average ratio is equal to 0.74 and 0.78, respectively; conversely, in the last period the average ratio decreases down to 0.48 (but also down to 0.25 for single-hour ratio), confirming that the dust from the deserts is mainly composed with coarse particles. It is noticed that sometimes (around 10% during the whole period) the $PM_{2.5}/PM_{10}$ ratio reaches or even exceeds 1, especially occurring in raining periods. Negative artifacts (i.e., loss of mass) are because of the internal heating mechanism of the TEOM monitor ($PM_{10}$), which is reported in literature when particulate matter in the poultry houses possibly contains semi-volatile compounds and moisture due to high levels of relative humidity (RH) and gas pollutants. TEOM may cause losses in mass through volatilization (Li *et al.*, 2012).

The average, minimum, maximum concentrations, the standard deviation (STD) and coefficient of variation (CV) for the elements measured in this study are shown in Table 1. K, Ca and Fe record relatively high concentrations and occupy 15.2%, 7%, 7.5% respectively of the total mass of elements. Concentration of Au is very variable and only record values larger than zero when there was the sand storm from May 26th to 28th. Ga, Cr, V are also high variances with coefficient of variation larger than 1. Zhang *et al.* investigated the chemical characteristics of $PM_{2.5}$ during the spring in Wuhan in 2013, using data from two different sampling sites. Calcium and Gallium exhibited

**Table 1.** Statistics for concentrations of the elements in $PM_{2.5}$ (ng $m^{-3}$).

| | Range | Mean ± STD | CV |
|---|---|---|---|
| K | 489.51–20,311.00 | 3,733.48 ± 3,249.17 | 0.87 |
| Ca | 136.22–11,187.00 | 1,792.49 ± 2,043.36 | 1.14 |
| V | 0.00–58.63 | 6.35 ± 9.01 | 1.42 |
| Cr | 0.29–103.51 | 9.81 ± 13.93 | 1.42 |
| Mn | 9.17–293.69 | 76.46 ± 50.94 | 0.64 |
| Fe | 247.71–7,685.00 | 1,820.76 ± 1,458.54 | 0.80 |
| Ni | 0.13–30.09 | 3.57 ± 3.39 | 0.95 |
| Cu | 3,88–191,63 | 30.13 ± 23.26 | 0.77 |
| Zn | 54.13–3,867.00 | 419.21 ± 388.18 | 0.93 |
| Ga | 0.00–4.21 | 0.37 ± 0.62 | 1.67 |
| As | 1.27–160.67 | 27.82 ± 27.91 | 1.00 |
| Se | 1.03–44.11 | 11.41 ± 8.10 | 0.71 |
| Ag | 0.38–33.04 | 6.09 ± 3.68 | 0.60 |
| Co | 1.33–22.92 | 8.05 ± 3.51 | 0.44 |
| Ba | 11.40–431.12 | 103.15 ± 79.17 | 0.77 |
| Au | 0.00–2.24 | 0.06 ± 0.24 | 3.77 |
| Hg | 0.00–4.54 | 1.24 ± 0.84 | 0.68 |
| Pb | 25.06–598.02 | 180.79 ± 128.79 | 0.71 |

higher levels in their monitoring campaigns (Zhang *et al.*, 2015: 6360.00 ng $m^{-3}$ and 10.70 ng $m^{-3}$, 7810.00 ng $m^{-3}$ and 10.18 ng $m^{-3}$) than in this work (1792.49 ng $m^{-3}$ and 0.37 ng $m^{-3}$). In contrary, Barium shows a higher average concentration in our study (103.15 ng $m^{-3}$) than in the work of Zhang (44.86 ng $m^{-3}$ and 42.12 ng $m^{-3}$). Barium is one of the most important crustal elements and probably the desert dust in Wuhan sensitively affects its average concentration. Barium concentration during the days ($16^{th}$ to $24^{th}$) before of the storm event was about 70 ng $m^{-3}$.

In Beijing, the average concentrations of Calcium (1284.90 ng $m^{-3}$), Iron (1261.20 ng $m^{-3}$), Manganese (67.6 ng $m^{-3}$), Copper (41.6 ng $m^{-3}$), Arsenic (32.1 ng $m^{-3}$), Barium (93.8 ng $m^{-3}$) and Lead (126.4 ng $m^{-3}$) (Yu *et al.*, 2013) are the same order of size as those we found in Wuhan (respectively 1792.49 ng $m^{-3}$, 1820.76 ng $m^{-3}$, 79.46 ng $m^{-3}$, 30.13 ng $m^{-3}$, 27.82 ng $m^{-3}$, 103.15 ng $m^{-3}$, 180.79 ng $m^{-3}$).

The time series of the most interesting trace elements used for the interpretation of the PMF's factors are shown in the panels of Fig. 3, grouping elements with similar concentrations. In particular, it can be seen that Calcium, Iron and Vanadium have similar patterns to each other and to the trend of $PM_{10}$ and $PM_{2.5}$. Specifically on the day of the storm, they all display a pronounced increase. Calcium and Iron are referred to as major crustal elements (Mason and Moore, 1982). Potassium records three peaks on $18^{th}$, $21^{th}$ and $26^{th}$ of May, which are more than 3 times higher of the mean value, and it is the most useful tracer for biomass burning (Ryu *et al.*, 2007) as recorded on $18^{th}$ and $21^{th}$, which is also recognized as crustal origin (Maria, 2014) as recorded on $26^{th}$.

### *Enrichment Factor*

Enrichment factor was determined to identify whether the presence of certain element in particle matter was primarily due to natural or anthropogenic processes. According to the results shown in Fig. 4, the mean EFs of Ca, Ba, K, Mn, V and Cr are below 10, which suggest that these elements would be more likely originated from natural sources such as crustal soil and re-suspended soil and have no obvious enrichment in particle matter (Xu *et al.*, 2013b). It is worth to notice for K the 90% percentage is over 10, and there are outliers over 10, and K is associated to biomass burning as reported in many other studies (e.g., Hleis *et al.*, 2013; Almeida *et al.*, 2015). Zn has different range of enrichment factor with the mean of 164.46 (Fig. 4 right axis), which is associated with activities mainly originated from anthropogenic sources such as traffic and industrial emission (Banerjee *et al.*, 2015). Previous study by Zhang *et al.* (2015) collected 24-h $PM_{2.5}$ samples every sixth day in Wuhan from August 2012 to July 2013, and the results about the EFs are traceable. It was also found that the EFs of Ba, Mn, and K were below 10, and the EF of Zn were above 10, which is consistant with the finding of Jiang *et al.* (2017) in China.

### *Source Identification and Apportionment by PMF*

Four factors are identified using PMF 5.0. Fig. 5 shows the percentage of the species in each factor.

The first factor, with high loading of K (87.56%), is attributed to biomass burning. In fact, Potassium was used as an unambiguous tracer of biomass burning (Begum *et al.*, 2007; Ryu *et al.*, 2007; Belis *et al.*, 2011; Yu *et al.*, 2013). This factor accounts for 62.3% of the total $PM_{2.5}$ mass and 22.9% of the total elements. The dominant contribution of $PM_{2.5}$ from biomass burning during May, when there was no evidence of open fires and agriculture waste burning, could be the emissions from the electricity power plants using bio-waste burning and bio-related cooking activities. The time series of the contribution for four factors are shown in Fig. 6, indicating that factor one peaked during the first period and the night of $26^{th}$. The first peak of factor one denotes that when $PM_{2.5}$ dominated in $PM_{10}$, it was mainly from local sources.

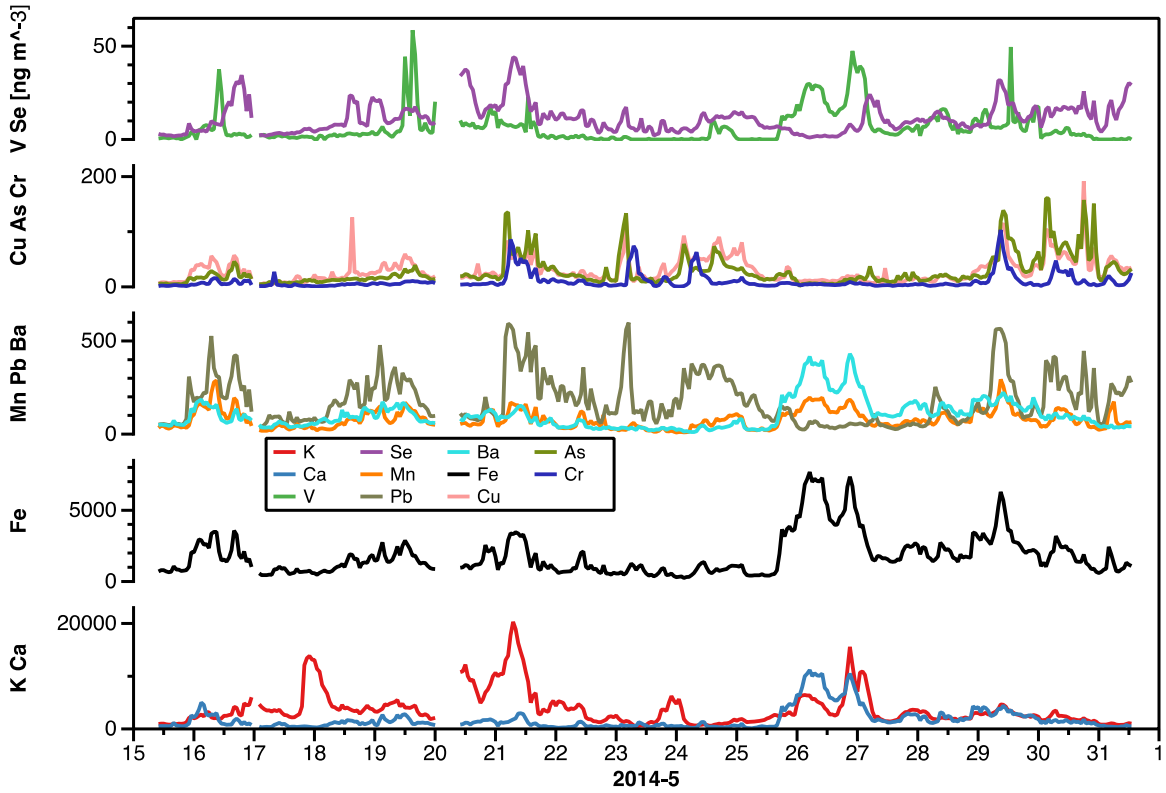


**Fig. 3.** Time series of the most interesting and trace elements in May 2014 (data missing from 0:00 to 1:00 on 17th, and from 1:00 to 9:00 on 20th due to power supply fail).

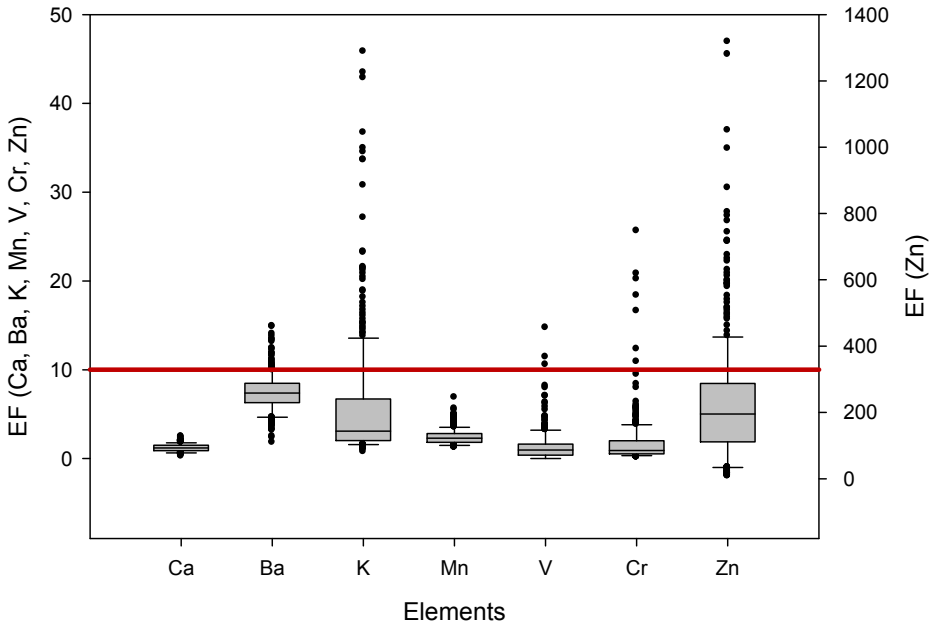


**Fig. 4.** Box plot for the EFs of the elements. The boundary of the box closest indicates the 25th and 75th percentile; error bars above and below the box indicate the 90th and 10th percentiles and the points show all outlines. The red line is at 10.

The second factor is characterized by high concentrations of As (93.06%), Cu (68.89%), Se (61.63%) and Pb (54.20%). Supporting by Han *et al.* (2015), these elements might be mainly from the industrial emissions, such as metallurgical processes. As and Se are mainly emitted by coal combustion (Thurston, *et al.*, 2011). Cu and Pb are typical tracers of metal and steel industries (Arruti *et al.*, 2011). Therefore, the factor, assigned as metallurgical and steel industries, contributes for 14% of the $PM_{2.5}$ mass and 29.4% of the total elements. There are a lot of industrial

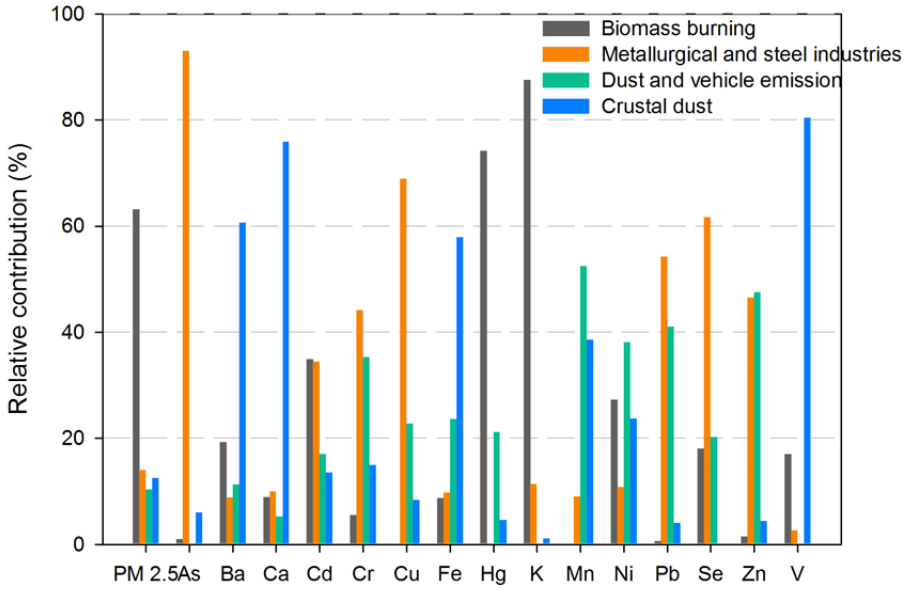


**Fig. 5.** Source profiles of $PM_{2.5}$ from PMF 5.0.

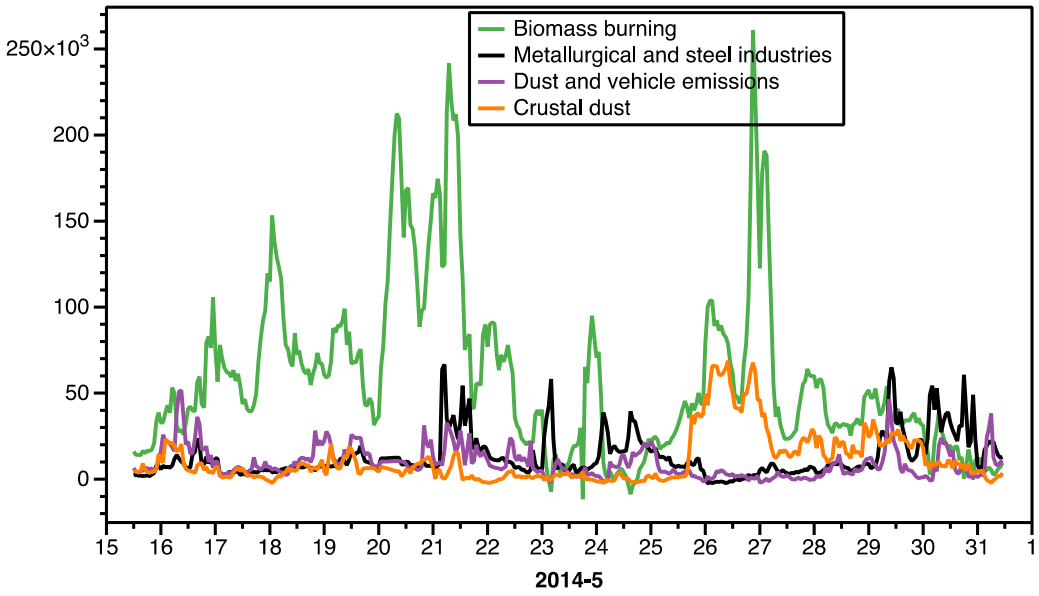


**Fig. 6.** Time serials of PMF contribution for four factors in May 2014.

companies in Wuhan, including the famous Wuhan iron and steel company, which has the approximate productivity of about 30 million t $year^{-1}$.

The third factor identified from PMF analysis is a source related to dust and vehicle emissions. This factor consists large fraction of Mn (49.93%), Zn (52.44%), Cr (35.29%), Cu (22.75%). Cr, Cu and Zn are tracers of traffic (Bozlaker *et al.*, 2014; Manousakas *et al.*, 2015). Cu and Zn are major additives to lubricating oils (Gugamsetty *et al.*, 2012); Zn and Mn emissions are also linked to other transportation activities such as brake and tire wear (Yu *et al.*, 2013). It was also reported by Canepari *et al.* (2008) that particles emitted from the asphalt pavement were characterized mainly by high concentrations of Zn, Cu, Cr, Ni, As and Pb. This emissions accounts for 10.4% of the $PM_{2.5}$ mass and 20.8% of the total elements. The vehicles are more than 100 million in Wuhan. The contribution of fine particles from vehicular emissions is evidenced and would accumulate during stable atmospheric conditions, for example, on the days of 16$^{th}$ and 21$^{th}$ of May.

The last factor is characterized by Ca (75.86%), Ba (60.59%), Fe (57.89%) and Mn (38.58%) which are the mainly crustal elements. The source can be associated with crustal dust. According to Wang *et al.*(2012), dust is an important contributor to $PM_{2.5}$, accounting for more than 25% of $PM_{2.5}$ mass concentration in urban areas. Soil resuspension is likely to be affected by Gobi or Thaklamakan dust events, which are known to influence particulate matter in Wuhan during 26$^{th}$ May (Figs. 2 and 6). The percentage contribution to the $PM_{2.5}$ is 12.5%, and to total elements is

26.8%. However, in this source, V contributes with 80.37%. V is a metal element which definitely originates from oil combustion (Querol *et al.*, 2002; Enamorado-Báez *et al.*, 2015). This phenomena is reasonable because the dust storm, occurred in Wuhan, has passed more than five provinces and brought not only dust but also contaminated particles when the air mass passing through industrial areas.

Chen *et al.*(2012) found that the source contribution to $PM_{2.5}$ in Wuhan is vehicle (27.1%), secondly sulfate and nitrate, industry (26.4%) and biomass burning (19.6%) by analysis the measurement from July 2011 to February 2012, showing different $PM_{2.5}$ contributions from our study. We conducted the observation during non domestic heating and air conditioning (cooling) period, secondary particles formed from unspecified pollution sources of human activity are not included.

After identifying the sources and analyzing their features for denomination, it is significant to seek conclusive confirmation of practical results to substantiate the corresponding argument. Thus, the R-programming was used to draw polar plots in consideration with the time series of the four identified sources. The profile information of the sources matches with the direction (along the axes Cartesian) and the speed (radial direction) of the wind.

The results are shown in Fig. 7. The greatest presence of the source named biomass burning is at South-West (SW) compared to the Super Monitoring Station of Wuhan, which is in the origin of the axes (Fig. 7(a)). The contribution of metallurgical and steel industries comes between ESE and SE compared to the sampling site (Fig. 7(b)) while the dust and vehicle emissions come between NNE and ESE (Fig. 7(c). The fourth source, defined as crustal dust, shows the highest concentrations coming between NNW and WS. The consistency in directions implies that the dust storm during 26$^{th}$ May has brought desert crustal material from the northwest/west-northwest, i.e., from the Gobi or the Taklamakan desert, in accordance with the contribution of the fourth source.

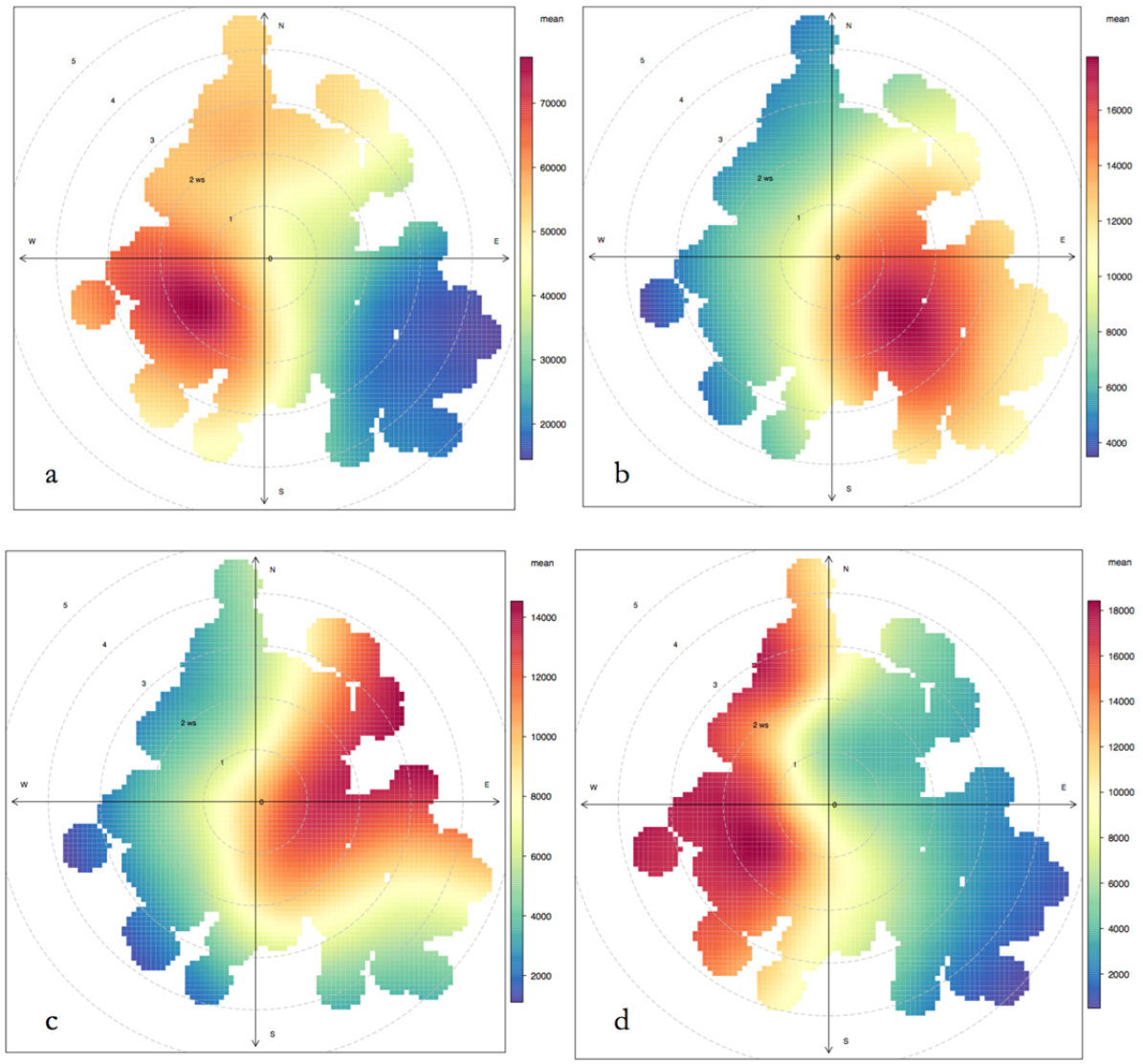


**Fig. 7.** Polar Plot for the four sources: a) biomass burning b) metallurgical and steel industries c) dust and vehicle emissions d) crustal dust. The graphs are generated using Openair in R programming (Carslaw and Ropkins, 2012; Carslaw, 2015).

## CONCLUSIONS

In this study, the characteristics of fine particulates ($PM_{2.5}$) in Wuhan, including concentration, composition (metal elements) and source identification, were investigated with hourly time resolution during a spring observation period (15th May, 2014–31st May, 2014).

From the results of Enrichment Factors (EFs), it could be concluded that Ca, Ba, Mn, V and Cr would be originated from natural sources. The EF of Zincs was far above 10 (164), revealing it is from anthropogenic sources and enriches in aerosols.

$PM_{2.5}$ sources were analyzed by employing the Positive Matrix Factorization (PMF) model. PMF analysis indicated four dominant sources, with the sequencing order of biomass burning, metallurgical and steel industries, dust and vehicle emissions, and crustal dust. Biomass burning was identified the largest contributor to $PM_{2.5}$ mass concentrations (62.3%) in the observation period without domestic heating and cooling. Power plants using bio-waste burning and bio-related cooking activities might be the main emission sources during non open fires and argriculture waste burning period in May in Wuhan. The origin of the biomass burning is SW (Fig. 6) where the Guodingshang garbage power plant located only 9 km from the station. There are five garbage power plants in the urban area of Wuhan, and four of them started to operate from 2014 including the near one. The results are novel and valuable to improve the knowledge of environment effect of bio-waste burning power plant and meaningful for the strategy of local air quality mitigation. The factor, assigned as metallurgical and steel industries, contributes with 14%, followed by crustal dust (12.5%) and dust and vehicle emissions (10.4%). An important observation emphasized that the dust storm carried not only large amounts of mineral dust but also metal elements such as Vanadium during the dust event (26th May) along the storm passage through the cities.

## ACKNOWLEDGMENTS

The financial support by State Environmental Protection Key Laboratory of Sources and Control of Air Pollution Complex (No.SCAPC201404) and Politecnico di Milano international fellowship grant are acknowledged. We also acknowledge the authors of the open source R program. (R Core Team, 2015).

## REFERENCES

Almeida, S.M., Lage, J., Fernández, B., Garcia, S., Reis, M.A. and Chaves, P.C. (2015). Chemical characterization of atmospheric particles and source apportionment in the vicinity of a steelmaking industry. *Sci. Total Environ*. 521–522: 411–420.

Arruti, A., Fernandez, O.I. and Irabien, A. (2011). Impact of the global economic crisis on metal levels in particulate matter (PM) at an urban area in the Cantabria Region (Northern Spain). *Environ. Pollut.* 159: 1129–1135.

Banerjee, T., Murari, V., Kumar, M. and Raju, M.P. (2015). Source apportionment of airborne particulates through receptor modeling: Indian scenario. *Atmos. Res*. 164–165: 167–187.

Begum, B.A., Biswas, S.K. and Hopke, P.K. (2007). Source apportionment of air particulate matter by chemical mass balance (CMB) and comparison with positive matrix factorization (PMF) model. *Aerosol Air Qual. Res*. 7: 446–468.

Belis, C.A., Cancelinha, J., Duane, M., Forcina, V., Pedroni, V., Passarella, R., Tanet, G., Douglas, K., Piazzalunga, A., Bolzacchini, E., Sangiorgi, G.M.L., Perrone, M.G., Ferrero, L., Fermo, P. and Larsen, B.R. (2011). Sources for PM air pollution in the Po Plain, Italy: A critical comparison of methods for estimating biomass burning contributions to benzo(a)pyrene. *Atmos. Environ.* 45: 7266–7275.

Bozlaker, A., Spada, N.J., Fraser, M.P. and Chellam, S. (2014). Elemental characterization of $PM_{2.5}$ and $PM_{10}$ emitted from light duty vehicles in the Washburn Tunnel of Houston, Texas: Release of rhodium, palladium, and platinum. *Environ. Sci. Technol.* 48: 54–62.

Canepari, S., Perrino, C., Olivieri, F. and, Astolfi, M.L. (2008). Characterisation of the traffic sources of PM through size-segregated sampling, sequential leaching and ICP analysis. *Atmos. Environ.* 42: 1088–1096.

Carslaw, D.C. (2015). *The openair manual-open-source tools for analyzing air pollution data*. Manual for version 1.1-4, King's College London.

Carslaw, D.C. and Ropkins, K. (2012). Openair - An R package for air quality data analysis. *Environ. Modell. Software* 27–28: 52–61.

Chatterjee, M., Silva Filho, E.V., Sarkar, S.K., Sella, S.M., Bhattacharya, A., Satpathy, K.K., Prasad, M.V., Chakraborty, S. and Bhattacharya, B.D. (2007). Distribution and possible source of trace elements in the sediment corse of a tropical macrotidal estuary and their ecotoxicological significance. *Environ. Int.* 33: 346–356.

Chen, H., Wang, Z., Feng, J., Chen, H. and Liu, J. (2012). Carbonaceous species composition and source apportionment of $PM_{2.5}$ in urban atmosphere of Wuhan. *Ecol. Environ. Sci.* 21: 1574–1579.

Cong, Z., Kawamura, K., Kang, S. and Fu, P. (2015). Penetration of biomass-burning emissions from South Asia through the Himalayas: New insights from atmospheric organic acids. *Sci. Rep.* 5: 9580.

Dordevic, D., Mihajlidi-Zelic, A. and Relic, D. (2005). Differentiation of the contribution of local resuspension from that of regional and remote sources on trace elements contenet in the atmospheric aerosol in the mediterranean area. *Atmos. Environ.* 39: 6271–6281.

Enamorado-Báez, S.M., Gómez-Guzmán, J.M., Chamizo, E. and Abril, J.M. (2015). Levels of 25 trace elements in high-volume air filter samples from Seville (2001–2002): Sources, enrichment factors and temporal variations. *Atmos. Res.* 155: 118–129.

Gao, J., Tian, H., Cheng, K., Lu, L., Wang, Y., Wu, Y., Zhu, C., Liu, K., Zhou, J., Liu, X., Chen, J. and Hao, J. (2014). Saesonal and spatial variation of trace elements in multi-size airborne particulate matters of Beijing, China:

Mass concentration, enrichment characteristics, source apportionment, chemical speciation and bioavailability. *Atmos. Environ.* 99: 257–265.

George, D.T., Kazuhiko, I. and Ramona, L. (2011). A source apportionment of U.S. fine particulate matter air pollution. *Atmos. Environ.* 45: 3924–3936.

Gugamsetty, B., Wei, H., Liu, C., Awasthi, A., Hsu, S., Tsai, C., Roam, G., Wu, Y. and Chen, C. (2012). Source characterization and apportionment of $PM_{10}$, $PM_{2.5}$ and $PM_{0.1}$ by using positive matrix factorization. *Aerosol Air Qual. Res.* 12: 476–491.

Han, L., Cheng, S., Zhuang, G., Ning, H. and Wang, H. (2015). The changes and long-range transport of $PM_{2.5}$ in Beijing in the past decade. *Atmos. Environ.* 110: 186–195.

Hleis, D., Fernandez-Olmo, I., Ledoux, F., Kfoury, A., Courcot, L., Desmonts, T. and Courcot, D. (2013). Chemical profile identification of fugitive and confined particle emissions from an integrated iron and steel making plant. *J. Hazard. Mater.* 250–251: 246–255.

Jiang, J., Zhou, W., Cheng, Z., Wang, S., He, K. and Hao, J. (2015). Particulate matter distributions in China during a winter period with frequent pollution episodes (January 2013). *Aerosol Air Qual. Res.* 15: 494–503.

Jiang, N., Dong, Z., Xu, Y., Yu, F., Yin, S., Zhang, R. and Tang, X. (2017). Characterization of $PM_{10}$ and $PM_{2.5}$ source profiles of fugitive dust in Zhengzhou, China. *Aerosol Air Qual. Res.*, *in Press*.

Johnson, K.S., de Foy, B., Zuberi, B., Molina, M.J., Xie, Y., Laskin, A. and Shutthanandan, V. (2006). Aerosol composition and source apportionment in Mexico City Metropolitan Area with PIXE/PESA/STIM and multivariate analysis. *Atmos. Chem. Phys*. 6: 4591–45600.

Kanakidou, M., Mihalopoulos, N., Kindap, T., Im, U., Vrekoussis, M., Gerasopoulos, E., Dermitzaki, E., Unal, A., Koçak, M., Markakis, K., Melas, D., Kouvarakis, G., Youssef, A.F., Richter, A., Hatzianastassiou, N., Hilboll, A., Ebojie, F., Wittrock, F., von Savigny, C., Burrows, J.P., Ladstaetter-Weissenmayer, A. and Moubasher, H. (2011). Megacities as hot spots of air pollution in the East Mediterranean. *Atmos. Environ.* 45: 1223–1235.

Karagulian, F., Belis, C.A., Dora, C.F.C., Prüss-Ustün, A.M., Bonjour, S., Adair-Rohani, H. and Amann, M. (2015).Contributions to cities' ambient particulate matter (PM): A systematic review of local source contributions at global level. *Atmos. Environ.* 120: 475–483.

Khan, M.F., Latif, M.T., Lim, C.H., Amil, N., Jaafar, S.A., Dominick, D., Mohd Nadzir, M.S., Sahani, M. and Tahir, N.M. (2015). Seasonal effect and source apportionment of polycyclic aromatic hydrocarbons in $PM_{2.5}$. *Atmos. Environ.* 106: 178–190.

Lang, J., Zhang, Y., Zhou, Y., Cheng, S., Chen, D., Guo, X., Chen, S., Li, X., Xing, X. and Wang, H. (2017). Trends of $PM_{2.5}$ and chemical composition in Beijing, 2000–2015. *Aerosol Air Qual. Res.* 17: 412–425.

Lazaridis, M., Eleftheriadis, K., Smolik, J., Colbeck, I., Kallos, G., Drossinos, Y., Zdimal, V., Vecera, Z., Mihalopoulos, N., Mikuska, P., Bryant, C., Housiadas, C., Spyridaki, A., Astitha, M. and Havranek, V. (2006). Dynamics of fine particles and photo-oxidants in the Eastern Mediterranean (SUB-AERO). *Atmos. Environ.* 40: 6214–6228.

Li, Q.F., Wang-Li, L., Liu, Z. And Heber, A.J. (2012). Field evaluation of particulate matter measurements using tapered element oscillating microbalance in a layer house. *J. Air Waste Manage. Assoc.* 62: 322–335.

Li, Y., Zhao, H. and Wu, Y. (2015). Characteristics of particulate matter during haze and fog (pollution) episodes over Northeast China, autumn 2013. *Aerosol Air Qual. Res.* 15: 853–864.

López, J.M., Callén, M.S., Murillo, R., García, T., Navarro, M.V., de la Cruz, M.T. and Mastral, A.M. (2005). Levels of selected metals in ambient air $PM_{10}$ in a urban sito of Zaragoza (Spain). *Environ. Res*. 99: 58–67.

Lu, H., Lin, S., Mwangi, J.K, Wang, L. and Lin, H. (2016). Characteristics and source apportionment of atmospheric $PM_{2.5}$ at a coastal city in Southern Taiwan. *Aerosol Air Qual. Res.* 16: 1022–1034.

Lv, B., Liu, Y., Yu, P., Zhang, B. and Bai, Y. (2015). Characterizations of $PM_{2.5}$ pollution pathways and sources analysis in four large cities in China. *Aerosol Air Qual. Res.* 15: 1836–1843.

Lyu, X.P., Wang, Z.W., Cheng, H.R., Zhang, F., Zhang, G., Wang, X.M., Ling, Z.H. and Wang, N. (2015). Chemical characteristics of submicron particulates ($PM_{10}$) in Wuhan, Central China. *Atmos. Res*. 161–162: 169–178.

Manoli, E., Voutsa, D. and Samara, C. (2002). Chemical characterization and source identification/apportionment of fine and coarse air particles in Thessaloniki. *Atmos. Environ.* 36: 949–961.

Manousakas, M., Diapouli, E., Papaefthymiou, H., Migliori, A., Karydas, A.G., Padilla-Alvarez, R., Bogovac, M., Kaiser, R.B., Jaksic, M., Bogdanovic-Radovic, I. and Eleftheriadis, K. (2015). Source apportionment by PMF on elemental concentrations obtained by PIXE analysis of $PM_{10}$ samples collected at the vicinity of lignite power plants and mines in Megalopolis, Greece. *Nucl. Instrum. Methods Phys. Res., Sect. B* 349: 114–124.

Marra Aranzazu, Revuelta (2014). Partitioning of magnetic particles in $PM_{10}$, $PM_{2.5}$ and $PM_1$ aerosols in the urban atmosphere of Barcelona (Spain). *Environ. Pollut*. 188: 109–117.

Mason, B. and Moore, C.B. (1982). *Principles of Geochemistry*. Wiley.

Pan, Y., Wang, Y., Sun, Y., Tian, S. and Cheng, M. (2013). Size-resolved aerosol trace elements at a rural mountainous site in Northern China: importance of regional transport. *Sci.Total Environ.* 461–462: 761–771.

Pan, Y., Tian, S., Li, X., Sun, Y., Li, Y., Wentworth, G.R. and Wang, Y. (2015). Trace elements in particulate matter from metropolitan regions of Northern China: Sources, concentrations and size distributions. *Sci. Total Environ.* 537: 9–22.

Polissar, A.V., Hopke, P.K., Paatero, P., Malm, W.C. and Sisler, J.F. (1998). Atmospheric aerosol over Alaska: 2. Elemental composition and sources. *Geophys. Res*. 103: 19045–19057.

Pope, C.A. and Dockery, D.W. (2006). Health effects of

fine particulate air pollution: Lines that connect. *J. Air Waste Manage. Assoc.* 56: 709–742.

Querol, X., Alastuey, A., de la Rosa, J., Sánchez-de-la-Campa, A., Plana, F. and Ruiz, C.R. (2002). Source apportionment analysis of atmospheric particulates in an industrialized urban site in southwestern Spain. *Atmos. Environ.* 36: 3113–3125.

Ryu, S.Y., Kwona, B.G., Kima, Y.J., Kimb, H.H. and Chunb, K.J. (2007). Characteristics of biomass burning aeroslo and its impact on regional air quality in the summer of 2003 at Gwangju Korea. *Atmos. Res*. 84: 362–373.

Samara, C. and Voutsa, D. (2005). Size distribution of airborne particulate matter and associated heavy metals in the roadside environment. *Chemosphere* 59: 1197–1206.

San Martini, F., Hasenkopf, C.A. and Roberts, D.C. (2015). Statistical analysis of $PM_{2.5}$ observations from diplomatic facilities in China. *Atmos. Environ.* 110: 174–185.

Srivastava, A., Gupta, S. and Jain, V.K. (2008). Source apportionment of total suspended particulate matter in coarse and fine size ranges over Delhi. *Aerosol Air Qual. Res.* 8: 188–200.

Tian, H., Wang, Y., Xue, Z., Qu, Y., Chai, F. and Hao, J. (2011). Atmospheric emissions estimation of Hg, As, and Se from coal-fired power plants in China. *Sci. Total Environ.* 409: 3078–3081.

US Environmental Potection Agency. PMF 5.0 User Guide.

US- Environmental Prtotection Agency. Xact 625 Guide.

Viana, M., Kuhlbusch, T.A.J., Querol, X., Alastuey, A., Harrison, R.M., Hopke, P.K., Winiwarter, W., Vallius, M., Szidat, S., Prévôt, A.S.H., Hueglin, C., Bloemen, H., Wåhlin, P., Vecchi, R., Miranda, A.I., Kasper-Giebl, A., Maenhaut, W. and Hitzenberger, R. (2008). Source apportionment of particulate matter in Europe: A review of methods and results. *J. Aerosol Sci.* 39: 827–849.

Wang, F., Zhong, Z., Wu, S., Zhang, W., Li, Q., Hu, S. and Wang, J. (2015). Case study of Wuhan dust pollution in May 2014. *Acta Sci. Natur. Univ. Pekinensis* 51: 1132–1140.

Wang, H., Tan, S.C., Wang, Y., Jiang, C., Shi, G.Y., Zhang, M.X. and Che, H.Z. (2014a). A multisource observation of the severe prolunged regional haze episode over eastern China in January 2013. *Atmos. Environ.* 89: 807–815.

Wang, L., Jang, C., Zhang, Y., Wang, K., Zhang, Q., Streets, D., Fu, J., Lei, Y., Schreifels, J., He, K., Hao, J., Lam, Y.F., Lin, J., Meskhidze, N., Voorhees, S., Evarts, D. and Phillips, S. (2010). A department assessment of air quality benefits from national air pollution control policies in China. Part I: Background, emission, scena matter rios and evaluation of meteorological prediction. *Atmos. Environ.* 44: 3442–3448.

Wang, L.C., Gong, W., Lin, A.W. and Hu, B. (2014b). Analysis of photosynthetically active radiation under various sky conditions in Central China. *Int. J. Biometeorol.* 58: 1711–1720.

Wang, Z.S., Wu, T., Shi, G.L., Fu, X., Tian, Y.Z. and Feng, Y.C. (2012). Potential source analysis for $PM_{10}$ and $PM_{2.5}$ in autumn in a northern city in China. *Aerosol Air Qual. Res.* 12: 39–48.

WHO (2001). Environment and People's Health in China.

Xu, H.M., Tao, J., Ho, S.S.H., Ho, K.F., Cao, J.J., Li, N., Chow, J.C., Wang, G.H., Han, Y.M., Zhang, R.J., Watson, J.G. and Zhang, J.Q. (2013a). Characteristics of fine particulate non-polar organic compounds in Guangzhou during the 16th Asian Games: Effectiveness of air pollution controls. *Atmos. Environ.* 76: 94–101.

Xu, L., Yu, Y., Yu, J., Chen, J., Niu, Z. and Yin, L. (2013b). Spatial distribution and sources identification of elements in $PM_{2.5}$ among the coastal city group in the Western Taiwan Strait region, China. *Sci. Total Environ.* 442: 77–85.

Yaroshevsky, A. (2006). Abundances of chemical elements in the Earth's crust. *Geochem. Int.* 44: 48–55.

Yu, L., Wang, G., Zhang, R., Zhang, L., Song, Y., Wu, B., Li, X., An, K. and Chu, J. (2013). Characterization and source apportionment of $PM_{2.5}$ in a urban environment in Beijing. *Aerosol Air Qual. Res.* 13: 574–583.

Zhang, F., Wang, Z., Cheng, H., Lv, X., Gong, W., Wang, X. and Zhang, G. (2015). Seasonal variations and chemical characteristics of $PM_{2.5}$ in Wuhan, central China. *Sci. Total Environ.* 518–519: 97–105.

Zhang, Z., Wang, F., Costabile, F., Allegrini, I., Liu, F. and Hong, W. (2012). Interpretation of ground-level ozone episodes with atmospheric stability index measurement. *Environ. Sci. Pollut. Res.* 19: 3421–3429.

*Received for review, June 20, 2017*
*Revised, August 23, 2017*
*Accepted, August 23, 2017*